

STRUCTURAL ALTERATION OF BENTONITE FROM NKALIKI BY ACID TREATMENT: STUDIES OF THE KINETICS AND PROPERTIES OF THE MODIFIED SAMPLES

Regina Obiageli Ajemba

Department of Chemical Engineering, Nnamdi Azikiwe University,
P. M. B. 5025, Awka, Anambra, Nigeria

ABSTRACT

Structural modification of clay minerals is necessary to improve their applicability. Bentonite from Nkaliki was treated with different concentrations of sulphuric acid ranging from 0.5 – 5.5mol/l to investigate the effects of acid activation on the structure and properties of the treated samples. The chemical compositions of the treated samples were analyzed using x-ray fluorescence, while the cation compositions of the liquid solution were analyzed with Atomic Absorption Spectrophotometer. The surface area, cation exchange capacity, and adsorption capacity were determined by conventional methods. The kinetics of the acid treatment reactions were studied by analyzing the data with established kinetic models. The chemical composition analysis revealed that the octahedral cations Al^{3+} , Fe^{3+} , and Mg^{2+} were leached out while the Si^{4+} increased as the acid concentration increased. The surface area and adsorption capacity of the treated samples increased to about four times that of the natural sample. Analysis of the experimental data showed that the removal of the cations of the octahedral and tetrahedral sheets followed the second-order homogeneous kinetic model and can be expressed as: $(1 - X)^{-1} - 1 = kt$; where X is the fraction of the cations removed at time t . The activation energy was calculated to be 33.16kJ/mol. This study has revealed that local bentonite from Nkaliki could be modified by acid activation to improve its application as sorbent in the vegetable oil processing industry.

KEYWORDS: Structural modification, Acid activation, Adsorption, Nkaliki bentonite, Kinetics, Octahedral cations.

I. INTRODUCTION

Bentonites, which contain high percentages of smectites, are greatly affected by thermal and acid treatments [1]. For instance, physicochemical properties, such as strength, swelling, plasticity, cohesion, compressibility, particle size, cation exchange capacity (CEC), pore structure, adsorptive properties, and catalytic activity as well as the chemical composition of the particles and the mineralogy can change considerably depending on thermal and acid effects [2 – 14]. Clay minerals vary in their chemical composition and this leads to varying mineralogical properties that include: layer charge, cation exchange capacity, adsorption capacity, and morphology [15]. Due to the large chemical composition variability, clay minerals are used in different industrial applications such as ceramics, food, chemical and paper industries. Sometimes, the clay minerals are used in their natural state and at other times after some specific modification [16]. One of such modification methods is acid treatment. Acid activation of clay mineral has been studied for years by many researchers [15, 17 – 22]. Different types of acid treatment have been described in the literature, varying from each other by the nature of the acid used, temperature, and intensity and time of the attack. Many authors have reported that the solids obtained, which are impure silica gels, keep the fibrous structure of the original clay material [18, 23]. This treatment modifies the surfaces of the clay minerals by dis-

aggregations of particles, possible elimination of mineral impurities, and removal of metal-exchange cations [22, 24]. The common commercial use of acid-activated clay minerals is bleaching or decolourations of oils [25] and in general in the field of adsorption and catalysis [26, 27]. Acid treated clay minerals are commercially used for the bleaching or decolourizing of oils because they exhibit wide range of chemical and physical properties depending on the extent of activation [28]. Acid activation of palygorskite revealed an important increase in the specific surface area [13] and increase in the number of acid centers and destruction of the silicate structure was also observed during the activation of a ferrous saponite [29]. These facts lead to the conclusion that, for a particular clay mineral, bleaching earth properties such as surface area and acidity should be optimized by properly controlling the activation conditions such as type and amount of acid, temperature, and treatment time [2, 30].

From the older studies of Osthaus [31] and Abdul-Latif and Weaver [17] to recent papers authors have studied the dissolution processes of silicates from the kinetic aspects, especially for Mg (II) cations, showing that the diffusion of the protons into the pores with planar or cylindrical geometries is the limiting step of the reaction. Indeed, when this process has taken over, the chemical reaction becomes instantaneous, being of first-order with respect to the metal cation and acid concentration.

In this work, the structure of bentonite from Nkaliki was altered by acid treatment and subsequent analyses were performed on the treated samples to investigate the effects of the acid dissolution reaction. Also, a kinetic model was applied to the data from the analysis of the liquids obtained after washing the different solids.

II. EXPERIMENTAL

Materials

The clay mineral used in this work was mined from the site located at Nkaliki (N: 9° 50' 00"; E: 9° 60' 55"; Altitude: 443m) in Ebonyi, Nigeria. The clay was wet and was sun-dried for three days before grinding with pestle and mortar. The palm oil was bought from a local mill located at Isuofia (N: 6° 1' 60"; E: 7° 2' 60"; Altitude: 361m) in Aguata, Anambra, Nigeria. All the other chemicals used were of analytical grade purchased at Conraws Company, Enugu.

Methods

Acid Activation

The dried and grinded clay samples were sieved to 0.212 mm particle size. The sized samples were reacted with different concentrations (0.5, 1.5, 2.5, 3.5, 4.5, and 5.5 mol/l) of sulphuric acid solution in the following manner. 10 g of the sized fraction was weighed out and reacted with already determined volume of the acid solution in a 250 ml bottomed flask. The flask and its contents were heated to a fixed temperature of 70°C while on a magnetic stirring plate and stirring was continued throughout the reaction duration. After the reaction time was completed, the suspension was immediately filtered to separate un-dissolved materials, washed three times with distilled water. The filtrate and washings were continued to a constant volume of 250 ml in a volumetric flask. The resulting solutions were diluted and analyzed for aluminum, magnesium, and iron ions using MS Atomic Absorption Spectrophotometer. The residue was also collected, washed to neutrality with distilled water, air dried and oven dried at 60°C and labeled as NK0, NK0.5, NK1.5, NK2.5, NK3.5, NK4.5, and NK5.5, where the numbers denote the acid concentration used in the activation process. To study the kinetics of the dissolution process of the octahedral ions- aluminium, magnesium, and iron, the activation was repeated at different time ranges of 0.5 to 6 hours.

Characterization

The chemical and mineralogical compositions of the natural and activated clay samples were determined. The chemical composition was determined using X-ray fluorescence (XRF), Philips PW 2400 XRF spectrometer; while the mineralogical composition was determined using Fourier transform infrared (FTIR), Shimadzu S8400 spectrophotometer, with samples prepared by the conventional KBr disc method. The surface area and cation exchange capacity of the treated and untreated samples were also determined in the following outlined methods:

Specific surface area

The surface area was determined using ethylene glycol mono-ethyl-ether (EGME) described by Carter et al [32, 33]. Clay samples were sun-dried and grinded to pass No. 40 sieve. A small amount of the sample was then placed in an oven at a temperature of 105 °C overnight to remove water and then dried with P₂O₅. One gram of the dried sample was spread into the bottom of aluminium tare and weighed (W_a) using an analytical balance with an accuracy of 0.001 g. Approximately 3.0 ml of laboratory grade EGME was added to the sample using a pipette and mixed together with a gentle swirling motion to create uniform slurry. All clay samples were covered with the EGME in order to obtain an accurate surface area measurement. The aluminium tare was then placed inside a standard laboratory glass sealed vacuum desiccator and allowed to equilibrate for 20 min. The desiccator was then evacuated using vacuum pump. The aluminium tare was removed from the desiccator and weighed (W_s) after a period of 12, 16, and 24 hours. When the mass of the sample varied by more than 0.001 grams between two measurements, the sample was placed back in the desiccator and evacuated again for an additional 2 hours. The process was continued until the sample mass did not vary by more than 0.001 g. The surface area was expressed as follows:

$$A = \frac{W_a}{0.000286W_s} \quad (1)$$

Where A = surface area, W_a = weight of EGME retained by the sample, W_s = weight of P₂O₅-dried sample, 0.000286 is the weight of EGME required to form uni-molecular layer on a square meter of the surface [34].

Cation Exchange Capacity (CEC) [35]

5 g of the clay sample was weighed into the 250 ml polythene bottle with a magnetic stirrer. The bottle and its contents were weighed (M_1). 100 ml of buffered barium chloride solution was added to the bottle and was placed on a magnetic stirring plate and agitated for 1 hour. At the end of the period, the bottle was centrifuged at 1500 rpm for 15 minutes and the supernatant was discarded. Further 200 ml of the buffered barium chloride solution was added and the mixture was agitated on a magnetic stirring plate for another 1 hour. The bottle and its contents were left overnight. The following day, the bottle and its contents were centrifuged at 1500 rpm for 15 minutes and the supernatant discarded. 200 ml of distilled water was added and agitated for few minutes on the magnetic stirring plate. It was centrifuged for further 15 minutes and the supernatant discarded. The bottle and its contents were weighed (M_2). 100 ml of MgSO₄ solution was pipette into the bottle and stirred well and was left to stand for 2 hours with occasional agitation on the magnetic stirring plate. After 2 hours the contents were centrifuged at 1500 rpm for 15 minutes and the supernatant decanted into the stoppered bottle. 5 ml aliquot of this solution was pipette into a 100 ml conical beaker and 5 ml of ammonia buffer and 6 drops of indicator were added to it. This mixture was titrated with standard EDTA (titer A_1 ml). Another titration was done with a 5 ml of aliquot of 0.05 M MgSO₄ solution (titer B ml). The end point was indicated by a blue to pink colour change. The Cation Exchange Capacity was calculated as follows:

$$CEC = 8 \left\{ B - \frac{(A_1 \times (100 + M_2 - M_1))}{100} \right\} meq/100g \quad (2)$$

Where M_1 = weight of bottle plus dry content (g), M_2 = weight of bottle plus wet content (g), A_1 = titration end-point of sample (ml), and B = titration end-point of MgSO₄ solution (ml)

Adsorption Capacity Study

To investigate the adsorption capacity of the activated clay samples, they were used to bleach palm oil. The method has been presented in earlier publication [36].

III. RESULTS AND DISCUSSIONS

Characterization

The chemical compositions of the liquid filtrates after acid activation are shown in Table 1. The removal of the dioctahedral cations depends on their form and amount within the bentonite sample. They are present in small quantity as exchangeable cations. It was observed that Ca (II) was easily removed more than the others of Na (I) and K (I). The Calcium ion occurred as calcite which is easily soluble in acid medium, while the Na and K ions were present as feldspars that are resistant to acid

Table 1. Analysis of the filtrate: Percentage of cations removed by the different acid treatments, in relation to their content in the untreated bentonite, expressed in oxide form.

Acid concentration	Time(h)	Composition of the filtrate (%)					
		Al ₂ O ₃	Fe ₂ O ₃	MgO	Na ₂ O	CaO	K ₂ O
1.5	0.5	3.7	5.9	11.8	23.7	76.5	7.5
	2	8.6	10.4	17.5	27.9	79.9	13.9
	4	12.6	16.5	25.4	28.8	81.5	20.7
	6	21.7	25.4	31.9	29.5	84.9	28.5
	8	29.8	33.6	38.6	30.4	86.7	35.3
2.5	0.5	6.8	8.7	17.6	26.8	78.6	10.1
	2	13.8	17.6	26.9	29.6	82.8	19.5
	4	19.6	24.4	33.6	30.8	83.4	26.4
	6	28.4	34.9	41.5	31.7	84.5	37.3
	8	33.8	38.9	47.4	33.6	85.8	40.2
3.5	0.5	8.3	11.7	22.7	32.6	80.5	13.1
	2	17.9	21.7	37.9	36.8	84.4	23.5
	4	24.9	29.8	46.8	37.6	85.2	31.8
	6	31.7	37.6	57.9	38.5	86.7	39.4
	8	38.9	44.7	68.9	39.1	87.3	45.4
4.5	0.5	11.2	16.4	38.8	35.7	82.8	17.6
	2	19.5	24.1	53.6	39.7	84.3	25.4
	4	29.7	36.3	69.7	40.2	86.4	37.5
	6	37.5	42.8	77.2	40.7	87.7	44.1
	8	45.8	49.7	97.6	41.2	88.6	50.6
5.5	0.5	10.8	14.7	36.8	39.8	84.3	21.2
	2	17.8	22.6	50.7	44.7	86.8	29.5
	4	27.7	34.5	61.4	46.3	87.6	42.6
	6	35.9	40.6	74.8	47.1	88.5	54.3
	8	44.8	48.6	86.5	47.6	89.8	63.2

attack. The removal of the tri-octahedral cations of Al³⁺, Fe³⁺, and Mg²⁺, was observed to be dependent on the intensity of the acid attack, their removal increased as the acid concentration was increased until 4.5mol/l, and thereafter their removal decreased as the concentration increased to 5.5mol/l. The Mg²⁺ was easily removed at mild treatment of the acid reaching 97.6% at 4.5mol/l for 8 hours. The removal of Al³⁺ and Fe³⁺ were both slow with Fe³⁺ removed faster at the same treatment. This is in agreement with the findings of other authors [13]. The content of SiO₂ was observed to increase as the acid concentration increased to 4.5mol/l and decreased with further increase in concentration (Figure 1) and this could be due to the formation of mullite which protects the clay layers from further acid attack. The behaviour shown by the Al₂O₃, Fe₂O₃, and MgO (Table 2) contents with progressive acid treatment is related to the progressive dissolution of the clay mineral. The octahedral sheet destruction passes the cations into the solution, while the silica generated by the tetrahedral sheet remains in the solid phase due to its insolubility [37]. Pesquera et al [38] suggest that this free silica generated by the initial destruction of the tetrahedral sheet, is polymerized by the effect of such high acid concentration and is deposited on the undestroyed silicate fractions, thereby protecting it from further acid attack [22, 25].

Table 2: Chemical analysis of the natural and acid activated (solid residue) Nkaliki clay samples determined by x-ray fluorescence (XRF) [47]

Clay	Chemical composition (%)	SiO ₂ /[Al ₂ O ₃ +
------	--------------------------	---

samples	Al ₂ O ₃	SiO ₂	Fe ₂ O ₃	MgO	Na ₂ O	K ₂ O	TiO ₂	LOI	Total	Fe ₂ O ₃ + MgO]
NK0	24.5	52.3	10.8	3.78	0.96	0.61	2.56	4.27	99.78	1.34
NK1.5	22.43	57.4	6.7	1.23	0.74	0.32	1.57	1.97	98.05	1.89
NK2.5	19.4	63.5	4.8	0.64	0.48	0.17	1.05	1.27	92.77	2.56
NK3.5	15.7	66.2	2.9	0.31	0.24	0.11	0.75	0.88	87.89	3.52
NK4.5	12.8	72.4	1.8	0.19	0.13	0.07	0.58	0.62	84.12	4.90
NK5.5	9.6	75.9	1.2	0.01	0.01	0.04	0.41	0.32	79.57	6.94

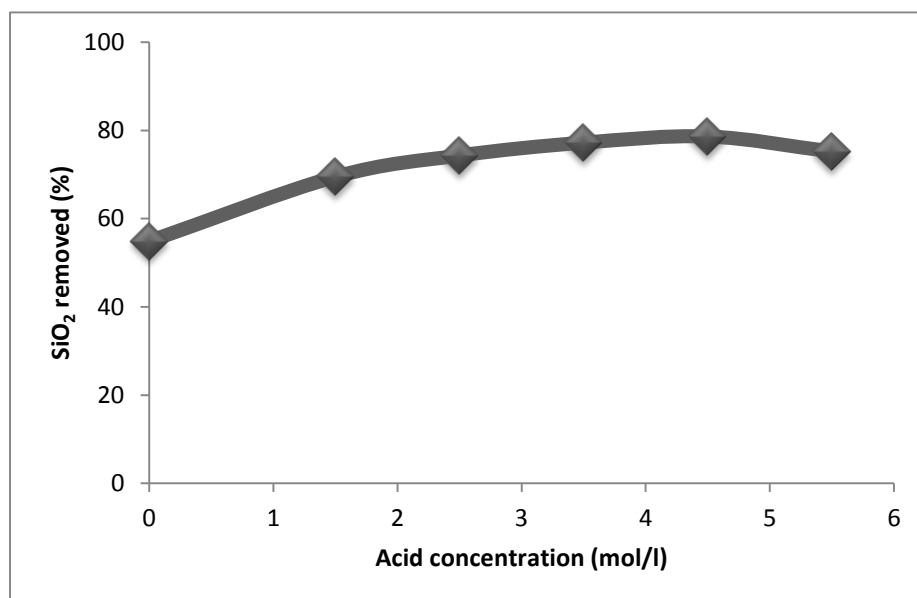


Figure 1: Plot of the SiO₂ removed from the clay samples at different acid concentrations.

Fourier transforms infrared (FTIR) spectroscopy analysis

The FTIR spectra of the raw and acid-leached clay samples were carried out in the range from 400 – 4000 cm⁻¹ to study the effect of acid-leaching on the clay mineral. The FTIR spectra of the raw and acid-leached samples are shown in Figures 2 and 3, respectively. The changes in the functional groups provide the indication of the modifications that occurred during the activation process. During the acid-leaching of the clay samples the protons from the acid medium penetrate into the clay structures attacking the OH groups thereby causing the alteration in the adsorption bands attributed to the OH vibrations and octahedral cations. The intensities of the stretching bands observed at 3623, 3432, 1641, and 920 cm⁻¹ (associated with O-H, along with Al-OH stretch) decreased after acid-activation. The increase in the severity of acid caused the disappearance of the stretching bands at 4660, 3694, 2376, and 998 cm⁻¹ assigned to the H-O-H stretching. The peak assigned to Si-O-Si stretch at 788 and 1066 cm⁻¹ remained after acid leaching, similar result was reported by others [39, 40]. The bands at 525, 690, and 998 cm⁻¹ associated to Si-O-Al vibration disappeared after the acid treatment of the clay sample. The transformation of the tetrahedral occurred at 788 cm⁻¹ which was increased after the acid treatment.

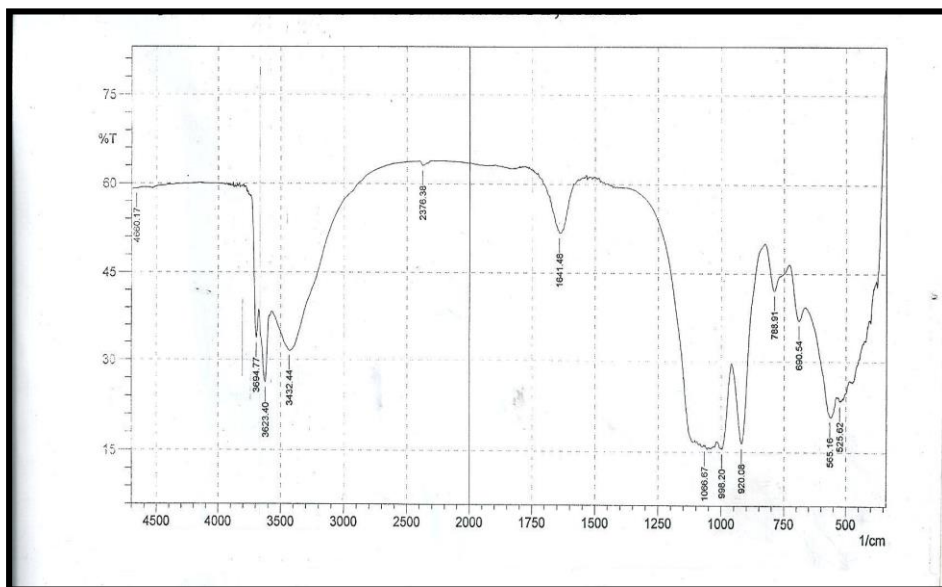


Figure 2: FT-IR spectra of natural Nkaliki bentonite [47].

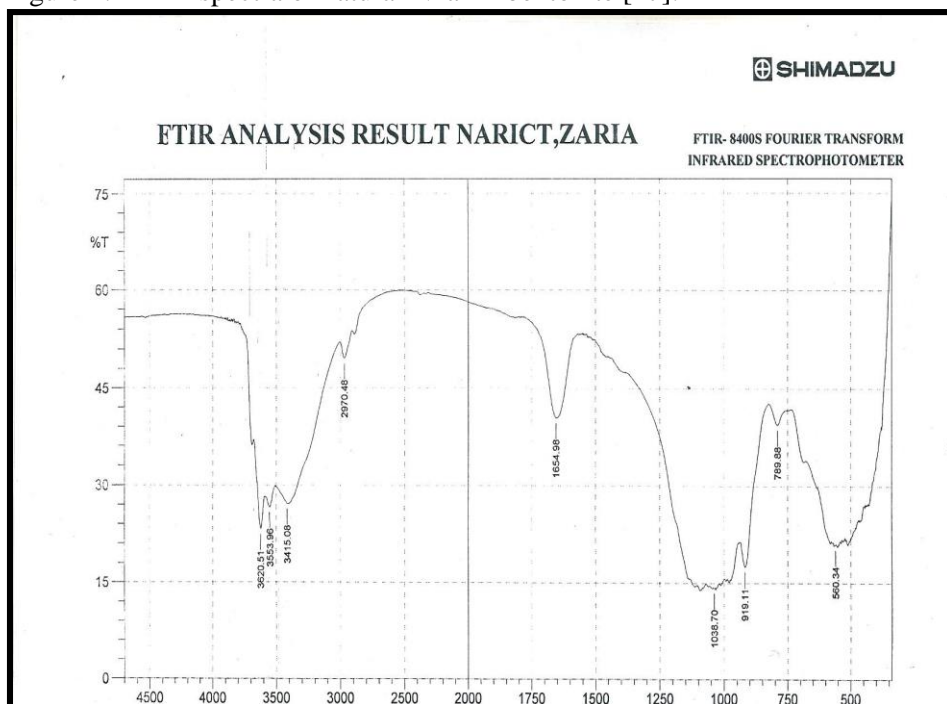


Figure 3: FT-IR spectra of acid-activated Nkaliki bentonite [47].

Surface area analysis

As the acid activation is increased, the surface area increased rapidly and reached a maximum and dropped. The increase in surface area is attributed to the removal of impurities, replacement of exchangeable cations (K^+ , Na^+ , and Ca^{2+}) with hydrogen ions, leaching of Al^{3+} , Fe^{3+} , and Mg^{2+} from the octahedral and tetrahedral sites which exposes the edges of the clay particles [41], de-lamination, and the generation of micro-porosity during the processes [37]. Further increase in the acid concentration beyond 4.5mol/l of H_2SO_4 showed a decrease in the surface area as shown in Figure 4. The decrease in surface area at higher acid concentrations is attributed to the deeper penetration of the acid into the voids and excessive leaching of Al^{3+} , Fe^{3+} , and Mg^{2+} , resulting in the collapse of the layered crystalline structure of the clay material [42] and it is also attributed to the polymerization of the generated free silica by the effect of excess acid concentration and is deposited on the surface of the clay particle preventing it from further attack [38].

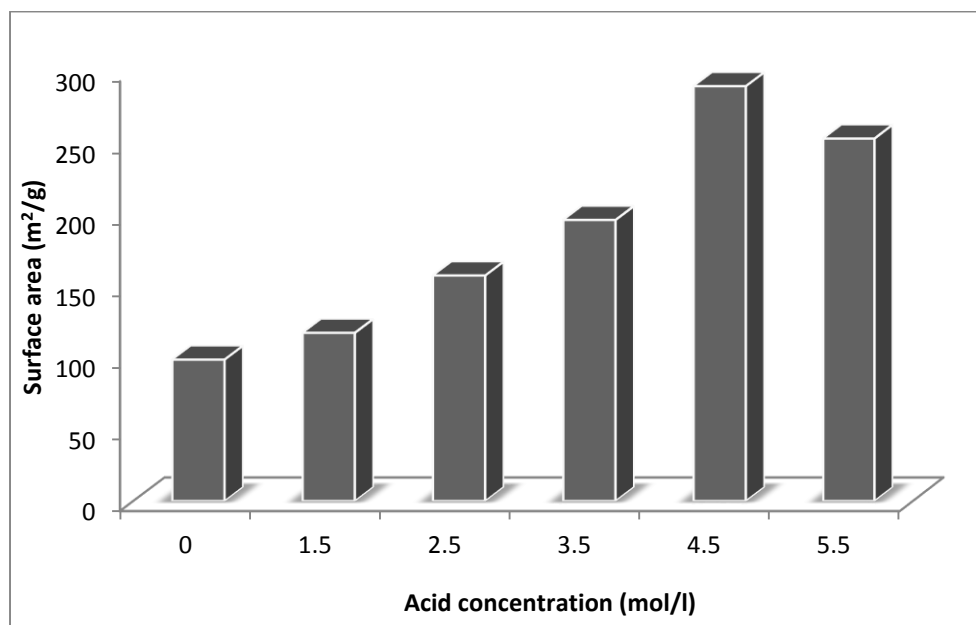


Figure 4: Plot of the surface areas of the natural and samples treated with different acid concentrations.

Cation exchange capacity (CEC)

The results of the cation exchange capacity of the activated samples show that the exchange ability of the activated samples decreased as the concentration of the acid used in the activation increased (Figure 5). This is due to the removal of the exchangeable ions from the lattice of the clay samples by the acid hydrogen ion which occupies the vacant sites created by the removal of the octahedral and tetrahedral ions. This progressive decrease in CEC values upon increase in the intensity of acid treatment could be also understood in terms of the leaching of the octahedral cations (Al^{3+} , Fe^{3+} , and Mg^{2+}) which results in a reduction of the negative layer charge and therefore of the CEC [43].

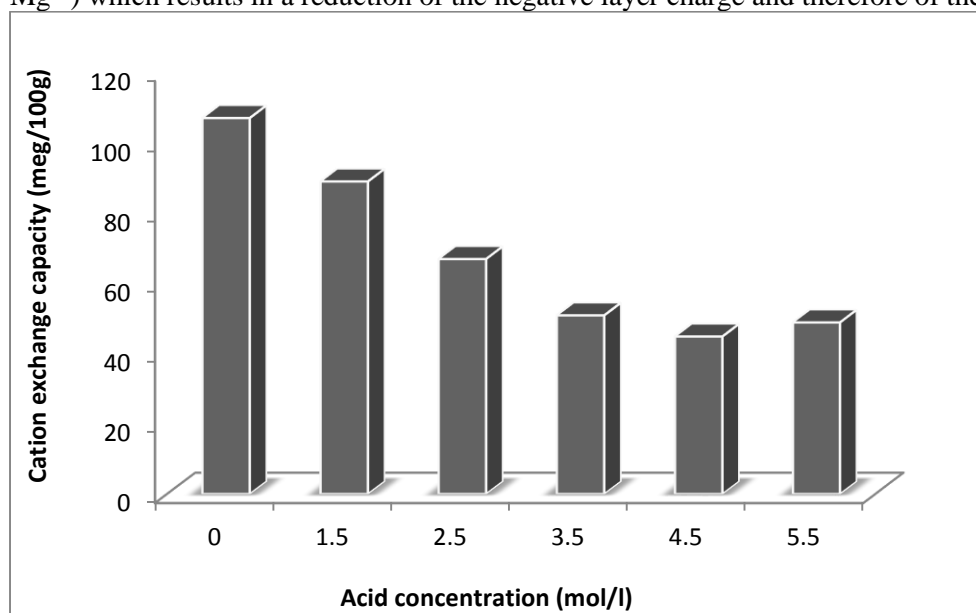
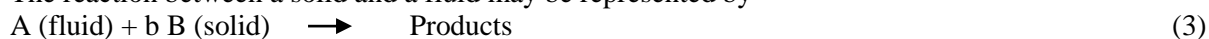


Figure 5: Plot of the cation exchange capacity of natural and samples treated at different acid concentrations.

Activation kinetics Studies

The reaction between a solid and a fluid may be represented by



The rate of reaction between a solid and a fluid can be expressed by heterogeneous and homogeneous reaction models. According to the shrinking-core model, the reaction is considered to take place at the outer surface of the un-reacted particle. When no ash forms, the reacting particle shrinks during reaction, and finally disappears. For a reaction of this kind, the following three steps are considered to occur in succession during reaction [44].

1. Diffusion of fluid reactant through the fluid layer to the surface of the solid.
2. Reaction of the fluid reactant and solid on the surface of the solid.
3. Diffusion of the products through the film layer to the bulk fluid.

The slowest of these sequenced steps is the rate-determining step. If the reaction is controlled by film diffusion, it becomes

$$X = [3bk_c C_A / \rho_B R_o] t = k_f t \quad (4)$$

If it is controlled by chemical reaction, it becomes

$$1 - (1 - X)^{1/3} = [bk_c C_A / \rho_B R_o] t = k_r t \quad (5)$$

The product layer diffusion control is given by

$$1 + 2(1 - X) - 3(1 - X)^{2/3} = [2M_B D C_A / \rho_B b R_o^2] t = k_d t \quad (6)$$

Where X is the fraction reacted, k_c is the kinetic constant, M_B is the molecular weight of the solid, C_A is the concentration of the dissolved lixiviant A in the bulk of the solution, b is the stoichiometric coefficient of the reagent in the leaching reaction, R_o is the initial radius of the solid particle, t is the reaction time, D is the diffusion coefficient in the porous product layer, ρ_B is the density of the solid particle, k_f , k_d , and k_r are the rate constants, respectively.

The experimental data were tested with the above kinetic models, but it was determined statistically that the dissolution reaction did not fit the models. The data were then analyzed by the second-order homogeneous kinetic model given by:

$$(1 - X)^{-1} - 1 = [2bk_s C_A / \rho_B R] t = k_s t \quad (7)$$

Using the equation, the plot of $[(1 - X)^{-1} - 1]$ versus time gave straight lines passing through the origin as shown in Figures 6 to 8 for Al^{3+} , Fe^{3+} , and Mg^{2+} , respectively. The coefficient of determination (R^2) values was used to determine the fitness of the data to the equation. As can be observed from the values of R^2 , it is evident that the fitness is close to unity for all the data sets from the experiment. The equation used in this present study is similar to those adopted by other authors. Corma et al [45] used $(1 - X)^2 = kt$, while Cetisli and Gedikbey [19] employed $[1 - (1 - X)^{1/2}]^2 = kt$, where x is the fraction of a cation dissolved at time t .

k_s from equation (7) is a pseudo-constant depending on the H^+ concentration and can be indicated by: $k_s = k [H^+]^\alpha$, where α is the reaction order. The reaction order can be calculated from the plots of the following equation;

$$\ln k_s = \ln k + \alpha \ln [H^+] \quad (8)$$

The values of α determined from the plots of $\ln k_s$ versus $\ln [H^+]$ (not shown here) for the dissolution of the octahedral cations were; 0.784 for Al^{3+} ; 0.920 for Fe^{3+} ; and 1.346 for Mg^{2+} . The values calculated for the dissolution of Al^{3+} and Fe^{3+} are different from that obtained by other authors [13, 45].

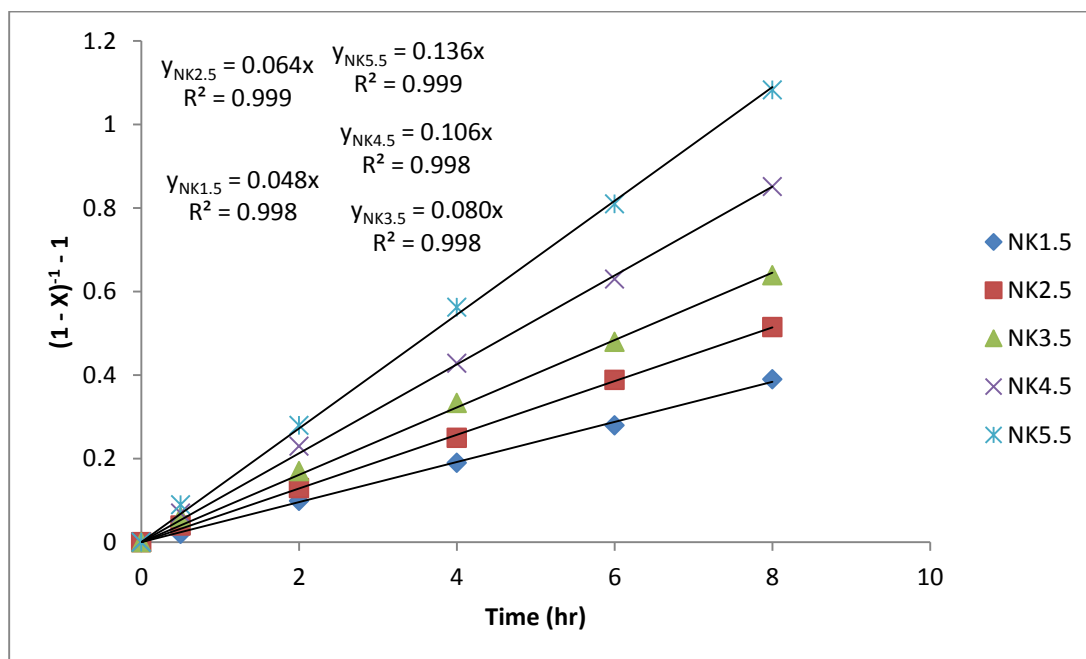


Figure 6: Plot of $[(1 - X)^{-1} - 1]$ versus time for Al^{3+} removed from the treated samples at different acid concentrations.

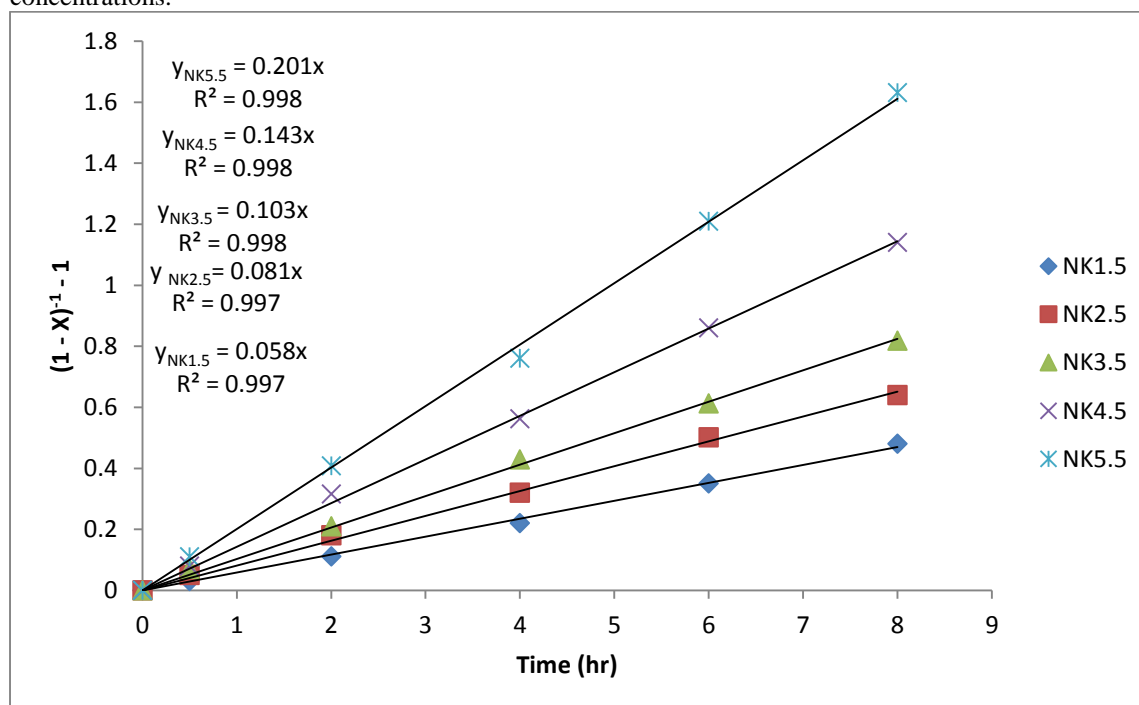


Figure 7: Plot of $[(1 - X)^{-1} - 1]$ versus time for Fe^{3+} removal from the treated samples at different acid concentrations.

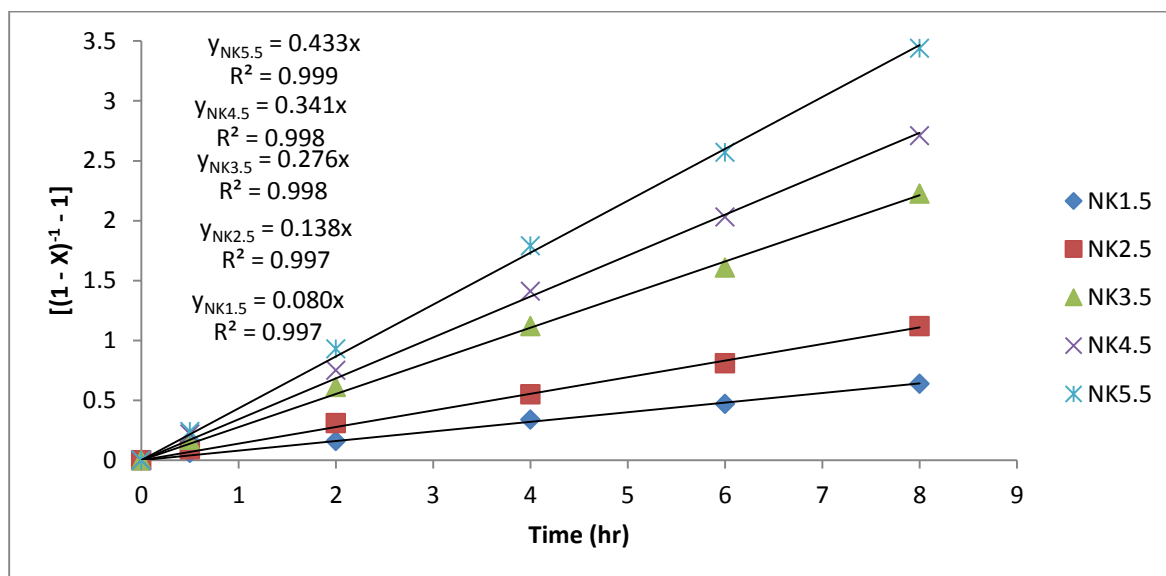


Figure 8: Plot of $[(1 - X)^{-1} - 1]$ versus time for Mg^{2+} removed from the treated samples at different acid concentrations.

Effect of temperature on activation

The effect of temperature on the rate of activation was investigated at 60, 80, 90, and 100 °C. The analysis shows that the activation rate has a linear relationship with the temperature as shown in Figure 9. The data of Figure 9 were fitted to the chemical reaction model and the data conformed to it and it is shown in Figure 10. The activation was observed to reach 45% at 100°C. This shows that the reaction is endothermic. At high temperature collision of the particles and the liquid molecules is enhanced. The relationship between the overall reaction rate constant and temperature according to the Arrhenius equation was employed in calculating the activation energy. The slope of the plot of Arrhenius equation was used to calculate the activation energy to be 33.16kJ/mol.

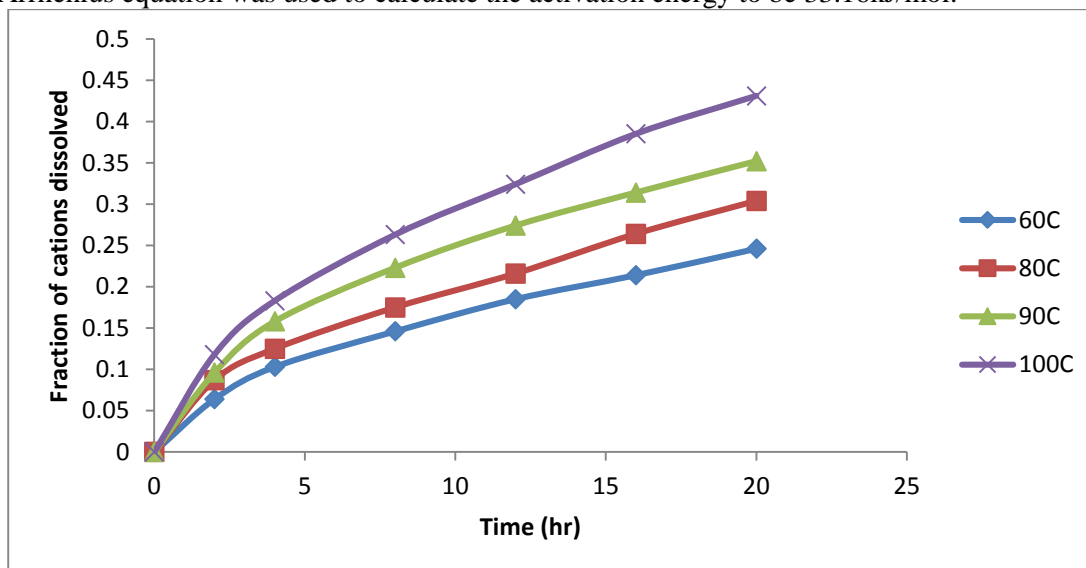


Figure 9: Plot of the fraction of cations removed from the 14mol/l activated Nkaliki bentonite at different temperatures.

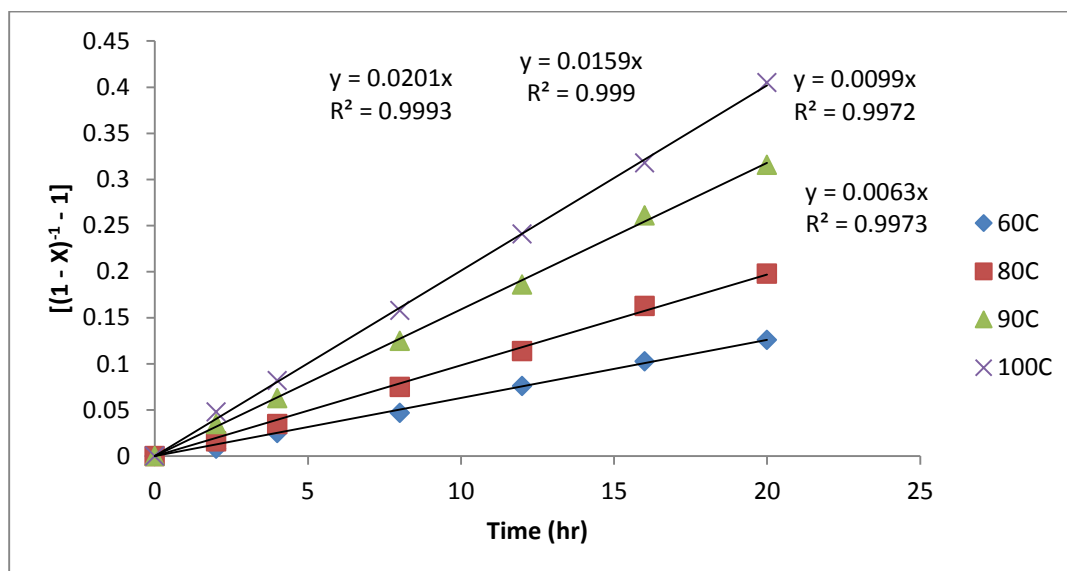


Figure 10: Plot of $((1 - X)^{-1} - 1)$ versus time for cations removal at different temperatures.

Adsorption performance studies

The results of the bleaching studies performed using the natural and acid-modified samples are depicted in Figure 11. The figure shows that the bleaching efficiency increased as the concentration of the acid used during the activation increased. This increase reached a maximum with the sample activated with 4.5mol/L of sulphuric acid and decreased as the concentration was increased to 5.5mol/L. This could be attributed to the fact that excess of the acid destroyed the crystalline structure of the clay and led to the decrease in surface area (Figure 2) and the ratio of SiO_2 to $[\text{Al}_2\text{O}_3 + \text{Fe}_2\text{O}_3 + \text{MgO}]$ [25, 38, 39, 43, 46].

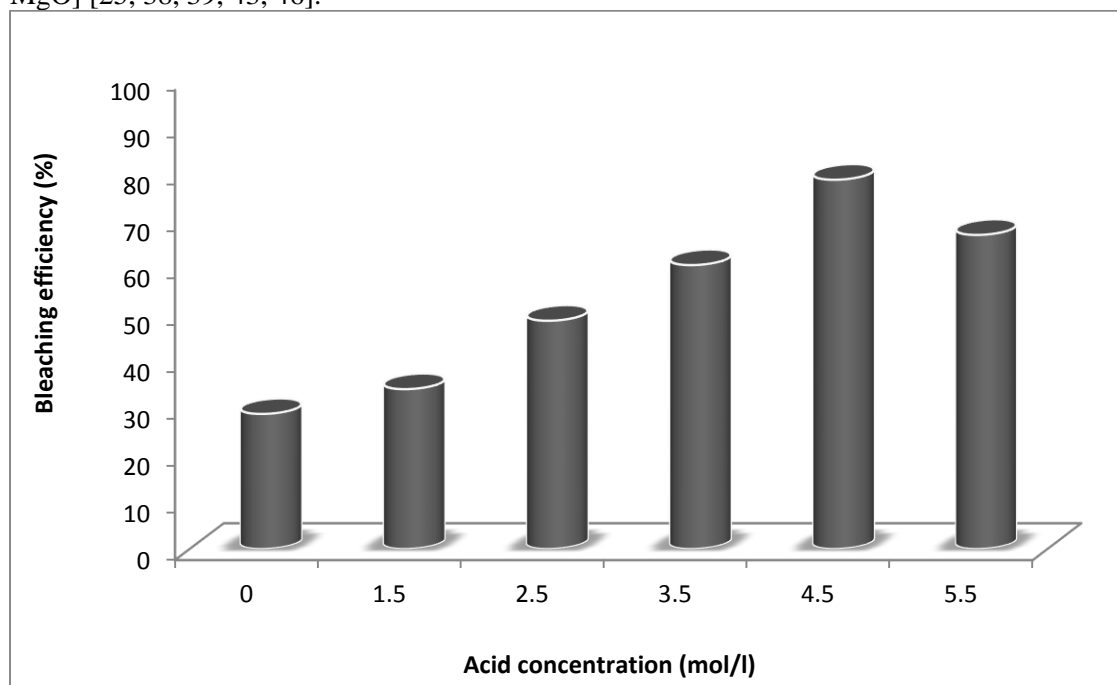


Figure 11: Bleaching efficiency of the clay samples activated at different acid concentrations.

IV. CONCLUSION

The structural alterations of bentonite from Nkaliki after treatment with different concentrations of sulphuric acid and kinetics of the process have been investigated in this work. The acid activation process resulted in the reorganization of the clay structures by the removal of the di- and tri-octahedral

cations (Al^{3+} , Fe^{3+} , Mg^{2+} , Na^+ , Ca^{2+} , and K^+) and subsequent modifications of the tetrahedral arrangement. These resulted to samples with increased surface area, adsorption capacity, and reduced cation exchange capacity. The order of the reaction determined with respect to the cations removed was; 0.784 for Al^{3+} ; 0.920 for Fe^{3+} ; and 1.346 for Mg^{2+} . The activation process could be described by the second-order homogeneous kinetic model with activation energy of 33.16kJ/mol.

LIST OF SYMBOLS/ABBREVIATIONS

A, surface area (m^2/g)
A1, titration end point (ml)
B, titration end point of solution (ml)
b, stoichiometric coefficient
CA, concentration of A (mol/l)
D, diffusion coefficient
kc, kinetic constant
kd, diffusion rate constant
kf, film rate constant
kr, reaction rate constant
MB, molecular weight of solid B
M1, weight of bottle plus dry content (g)
M2, weight of bottle plus wet content (g)
Ro, initial radius of solid particle
t, time of reaction, (s)
Wa, weight of EGME
Ws, weight of P_2O_5 dried sample
X, fraction reacted at time *t*
α, reaction order
ρB, density of solid

REFERENCES

- [1] Sarikaya, Y., Onal, M., Baran, B., and Alemdaroglu, T., "The effect of thermal treatment on some of the physicochemical properties of a bentonite," *Clays Clay Miner.*, 48 (5), pp. 557 – 562, 2000.
- [2] Breen, C., Zahoor, E. D., Madejova, J. and Komadel, P., "Characterization and catalytic activity of acid-treated, size-fractionated smectites," *J. Phys. Chem.*, B. 101, pp. 5324 – 5331, 1997.
- [3] Hymore, F. K., "Effects of some additives on the additives on the performance of acid activated clays in the bleaching of palm oil," *Appl. Clay Sci.*, 10, pp. 379 – 385, 1996.
- [4] Komadel, P., Schmidt, D., Madejova, J. and Ciel, B., "Alteration of smectite by treatments with hydrochloric acid and sodium carbonate solutions," *Appl. Clay Sci.*, 5, pp. 113 – 122, 1990.
- [5] Bradley, W. F. and Grim, R. E., "High temperature thermal effects of clay and related materials," *Am. Miner.*, 36, pp. 182 – 201, 1951.
- [6] Brindley, G. W., "Thermal reactions of clay and clay minerals," *Ceramica*, 24, pp. 217 – 224, 1978.
- [7] Kumar, P., Jasra R. V. and Bhat, T. S., "Evaluation of porosity and surface acidity in montmorillonite clay on acid activation," *Ind. Eng. Chem. Res.*, 34, pp. 1440 – 1448, 1995.
- [8] Mozas, T., Bruque, S. and Rodriguez, A., "Effect of thermal treatment on lanthanide montmorillonites: Dehydration," *Clay Miner.*, 15, pp. 421 – 428, 1980.
- [9] Reicle, W. T., "Catalytic reactions by thermally activated, synthetic, anionic clay minerals," *J. Catalysis*, 94, pp. 547 – 557, 1985.
- [10] Osthaus, B. B., "Kinetics studies on montmorillonite and nontronite by the acid dissolution technique," *Clays Clay Min.*, 4, pp. 301 – 311, 1956.
- [11] Ceylan, H., Yildiz, A. and Sarikaya, Y., "Investigation of adsorption of fatty acids on two different clays using IR, DTA and TGA techniques," *Turkish J. Chem.*, 17, pp. 267 – 272, 1993.
- [12] Sarikaya, Y., Ceylan, H., Bozdogan, I. and Akinc, M., "Determination of pore size distributions from thermal analysis data: Thermoporometry," *Turkish J. Chem.*, 17, pp. 119 – 124, 1993.
- [13] Vicente-Rodriguez, M. A., Lopez-Gonzalez, J. D., Banares-Munoz, M. A., Casado-Linarejos, J., "Acid activation of Spanish sepiolite II. Consideration of kinetics and physico-chemical modifications generated," *Clay Min.*, 30, pp. 315 – 324, 1995.
- [14] Joshi, R. C., Achari, G., Horfield, D. and Nagaraj, T. S., "Effects of heat treatment on strength of clays," *J. Geotech. Eng.*, 120, pp. 1080 – 1088, 1994.

- [15] Steudel, A., Batenburg, L., Fischer, H., Weidler, P. and Emmerich, K., "Alteration of swelling clay minerals by acid activation," *Appl. Clay Sci.*, 44, pp. 105 – 118, 2009.
- [16] Komadel, P., Madejova, J., Janek, M., Gates, W., Kirkpatrick, R. J. and Stucki, J. W., "Dissolution of hectorite in inorganic acids," *Clays Clay Min.*, 44, pp. 228 – 236, 1996.
- [17] Abdul-Latif, N. and Weaver, C., "Kinetics of acid dissolution of palygorskite (attapulgite) and sepiolite," *Clays Clay Miner.*, 17, pp. 169 – 176, 1969.
- [18] Bonilla, J., Lopez Gonzalez, J., Ramirez Saenz, A., Rodriguez Reinoso, F. and Valenzuela Calahorro, C., "Activation of a sepiolite with dilute solutions of HNO₃ and subsequent heat treatments II: Determination of surface acid centers," *Clay Miner.* 16, pp. 173 – 180, 1981.
- [19] Cetisli, H. and Gedikbey, T., "Dissolution kinetics of sepiolite from Eskisehir (Turkey) in hydrochloric and nitric acids," *Clay Miner.*, 25, pp. 207 – 215, 1990.
- [20] Rodriguez Reinoso, F., Ramirez Saenz, A., Lopez Gonzalez, J., Valenzuela Calahorro, C. and Zurita Herrera, L., "Activation of a sepiolite with dilute solutions of HNO₃ and subsequent heat treatments III: Development of porosity," *Clay Miner.*, 16, pp. 315 – 326, 1981.
- [21] Suarez, M., Flores, L. V. and Martin-Pozas, J. M., Textural study of palygorskite by acid treatment, *Abs. Med. Clay Meeting, Italy*, 132, 1992.
- [22] Vicente-Rodriguez, M. A., Lopez-Gonzalez, J. D. and Banares-Munoz, M. A., "Acid activation of a Spanish sepiolite: Physico-chemical characterization, free silica content and surface area of the solids obtained," *Clay Min.*, 29, pp. 361 – 370, 1994a.
- [23] Gonzalez, L., Ibarra, L., Rodriguez, A., Moya, J. and Valle, F., "Fibrous silica gel obtained from sepiolite by hydrochloric acid attack," *Clay Min.*, 19, pp. 93 – 109, 1984.
- [24] Vicente-Rodriguez, M. A., Suarez-Barrios, M., Lopez-Gonzalez, J. D. and Banares-Munoz, M. A., "Acid activation of a ferrous saponite (griffithite): Physico-chemical characterization and surface area of the products obtained," *Clays Clay Min.*, 42, pp. 724 – 733, 1994b.
- [25] Srasra, E., Bergaya, F., Vandamme, H. and Arigub, N. K., "Surface properties of an activated bentonite: Decolourization of rape-seed oils," *Appl. Clay Sci.*, 4, pp. 411 – 420, 1989.
- [26] Fahn, R. and Fenderl, K., "Reaction products of inorganic dye molecules with acid treated montmorillonite," *Clay Min.*, 18, pp. 447 – 458, 1983.
- [27] Mokaya, R. and Jones, W., "Pillared clays and pillared acid-activated clays: A comparative study of physical, acidic and catalytic properties," *J. Porous Mat.*, 6, pp. 335 – 344, 1995.
- [28] Boki, K., Kudo, M., Wada, T. and Tamura, T., "Bleaching of alkali-refined vegetable oils with clay minerals," *J. Am. Oil Chem. Soc.*, 69, pp. 232 – 236, 1992.
- [29] Motlagh M. M. K., Youzbashi A. A., and Rigi Z. A., "Effect of acid activation on structural and bleaching properties of a bentonite," *Iranian J. Mater. Sci. Eng.*, 8 (4), pp. 50 – 56, 2011.
- [30] Falaras, P., Kovanis, I., Lezou, F. and Seiragakis, G., "Cotton seed oil bleaching by acid-activated montmorillonite," *Clay Miner.*, 34, pp. 221 – 232, 1999.
- [31] Osthaus, B. B., "Chemical determination of tetrahedral ions in nontronite and montmorillonite," *Clays Clay Min.*, 2, pp. 404 – 412, 1954.
- [32] Carter, D. L., Mortland, M. M. and Kemper, W. D., Specific surface. *Methods of soil analysis*, Chapter 16, Agronomy, No. 9, Part 1, 2nd Ed., American Society of Agronomy, p. 456, 1964.
- [33] Carter, D. L., Heilman, M. D. and Gonzalez, C. L., "Ethylene Glycol Mono-ethyl Ether for determining surface area of silicate minerals," *Soil Sci.*, 100, pp. 356 – 364, 1965.
- [34] Chiou, C. T., Rutherford, D. W. and Manes, M., "Sorption of N₂ and EGME vapours on some soils, clays, and mineral oxides and determination of sample surface areas by use of sorption data," *Environ. Sci. Technol.*, 27, pp. 1587 – 1596, 1993.
- [35] Inglethorpe, S. D. J., Morgan, D. J., Highley, D. E. and Bloodworth, A. J., *Industrial mineral laboratory manual- Bentonite*, British Geological Survey Technical Report, WG/93/20, 1993.
- [36] Ajemba, R. O. and Onukwuli, O. D., "Evaluation of the effects of acid activation on adsorptive properties of clay from Ukpor in bleaching palm oil," *Int. J. Multi. Sci. Eng.*, 3 (5), pp. 46 – 52, 2012.
- [37] Dias, M. I., Suarez, M. B., Prates, S., and MartinPozas, J. M., "Characterization and acid activation of Portuguese special clays," *Clay Min.*, 38, pp. 537 – 544, 2003.
- [38] Pesquera, C., Gonzalez, F., Benito, I., Blanco, C., Mendioroz, S. and Pajares, J., "Passivation of a montmorillonite by the silica created in acid activation," *J. Mat. Chem.*, 2, pp. 907 – 917, 1992.
- [39] Christidis, G. E., Scott, P. W. and Dumham, A. C., "Acid activation and bleaching capacity of bentonites from the islands of Milos and Chios, Aegean and Greece," *Appl. Clay Sci.*, 12, pp. 329 – 338, 1997.
- [40] P. Komadel and J. Madejova, Acid Activation of Clay Minerals, in Bergaya F., Theng B. K., Lagaly G., (Ed.), *Handbook of Clay Science Vol. 1*, Elsevier Science Publishers Amsterdam-New York, p. 263, 2006.
- [41] Tsai, W. T., Hsu, H. S., Su, T. Y., Lin, K. Y., Lin, C. M. and Dai, T. H., "The adsorption of cationic dye from aqueous solution onto acid-activated andersite," *J. Hazard. Mat.*, 147, pp. 1056 – 1064, 2007.

- [42] Korichi, S., Elias, A. and Mefti, A., "Characterization of smectite after acid activation with microwave irradiation," *Appl. Clay Sci.*, 38, pp. 279 – 286, 2009.
- [43] Breen, C., Madejova, J. and Komadel, P., "Characterization of moderately acid-treated, size-fractionated montmorillonites using IR and MAS NMR spectroscopy and thermal analysis," *J. Mat. Chem.*, 5, pp. 469 – 478, 1995.
- [44] Levenspiel, O., *Chemical Reaction Engineering*, 2nd edition; John Wiley and Sons: New York, 256, 1972.
- [45] Corma, A., Mifsud, A., and Perez, J., "Studies of the acid activation of sepiolite: structural properties of the modified samples," *Clay Miner.* 21, pp. 69 – 84, 1986.
- [46] Myriam, M., Suarez, M., and MartinPozas, J. M., "Structural and textural modifications of palygorskite and sepiolite under acid treatment," *Clays Clay Min.*, 46, pp. 225 – 237, 1998.
- [47] Ajemba, R. O., "Thermodynamics and kinetics studies of the dissolution and adsorptive applications of Ukpör, Udi, and Nteje clays," Ph.D thesis, Nnamdi Azikiwe University, Nigeria, 2012.